Structural Engineering and Mechanics, Vol. 16, No. 1 (2003) 63-81
DOI: http://dx.doi.org/10.12989/sem.2003.16.1.063

Behaviour of volcanic pumice based thin walled composite filled columns under eccentric loading

Khandaker M. Anwar Hossain†

Department of Civil Engineering, Ryerson University, 350 Victoria Street, Toronto, Ontario, M5B 2K3, Canada

(Received September 9, 2002, Accepted April 28, 2003)

Abstract. This paper describes experimental and theoretical investigations on the behaviour of thin walled composite (TWC) filled columns under eccentric loading conditions. Details of the experimental investigation including description of the test columns, testing arrangements, failure modes, strain characteristics, load-deformation responses and effects of various geometric and material parameters are presented. The current paper also introduces the use and effect of lightweight Volcanic Pumice Concrete (VPC) in TWC columns. Analytical models for the design of columns under eccentric loading conditions have been developed taking into consideration the effect of confined concrete. The performance of design equations is validated through experimental results. The proposed design models are found to produce better results compared with available design procedures and Code based formulations. A computer program is developed to generate the interaction diagrams based on the proposed design equations that can be used for design purposes.

Key words: volcanic pumice; eccentric loading; confined concrete; composite columns; buckling; strength-interaction; design equation.

1. Introduction

Thin walled composite (TWC) filled columns comprise (Hossain 1998, 1999a, 2000, 2001) cold-formed steel section with an in-fill of concrete. A typical TWC column is shown in Fig. 1. The inherent advantages of this system are derived from its structural configurations. TWC columns do not require formwork in the construction stage and steel acts as reinforcement in the service stage. They are simple to fabricate and construct compared to conventional reinforced concrete where skilled workers are needed to cut and bend complex forms of reinforcement. The in-fill concrete in TWC sections is less likely to be affected by adverse temperature and winds as experienced in the case of reinforced concrete. However, some problems include: low fire resistance capacities (though thermal capacity of concrete may provide some resistance); the possibility of column bursting due to freezing and the possible need for factory filling of smaller sections to avoid voids developing. In most cases, the geometry of proprietary hot rolled steel tubes has been found to be such that local buckling is avoided (Wright 1993, 1995). Concrete filled steel elements as a means of providing aesthetic and economical structural elements attract much interest in the construction industry.

† Doctor

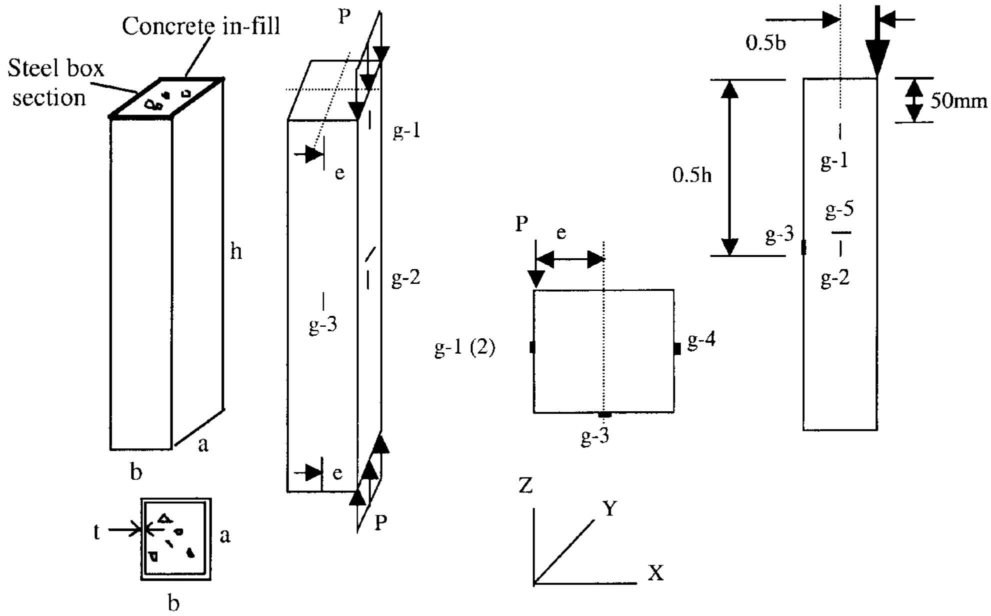

Fig. 1 Schematic and instrumentation of eccentrically loaded TWC columns

Earlier research was concentrated mainly on reinforced concrete and encased composite columns. Most of the works on filled columns were on axially loaded circular hollow section (CHS) columns (Neogi *et al.* 1969) with limited work on axial rectangular hollow section (RHS) (Shakir-Khalil and Zeghiche 1989, Shakir-Khalil and Mouli 1990), square hollow section (SHS) and eccentric filled columns. Neogi *et al.* (1969) conducted experimental and numerical works on filled CHS columns under the effect of axial and eccentric loads with special reference to the augmentation effect on their load carrying capacity.

Shakir-Khalil and Zeghiche (1989) and Shakir-Khalil and Mouli (1990) investigated filled RHS columns subjected to axial and both uniaxial and biaxial eccentric loads. Tests confirmed the unsafe results of columns under uniaxial bending about the minor axes compared with BS5400 (1979) predictions. However conclusions on biaxial bending were not conclusive due to the limited number of tests conducted.

Wright (1993, 1995) conducted investigations on the buckling pattern of concrete filled and encased steel sections under bending, axial and shear loading. He proposed design equations for the slenderness limit of plates in contact with a rigid medium. The limits in the codes of practice were deemed too conservative for such plates since its buckling potential is substantially reduced. The structural benefits of filling and encasing such as buckling capacity, strength and ductility, are possible only after careful designs are conducted. The combined and individual effect of axial and bending (uniaxial) was numerically modeled (Wright and Hossain 1995). The use of the energy method was presented and buckling stress derivations for filled and unfilled sections for a particular stress level, including elastic and plastic buckling stress derivation was described.

Wang and Moore (1997) and Wang (1999) investigated composite RHS columns subjected to eccentric (uniaxial and biaxial) loading and proposed a suitable simple design procedure based on the standard recommendation (BS5950 1988). However, the discrepancies between the codes of practice predictions and the proposed method increased for slender columns with end eccentricities. Due to a lack of experimental data, the problem could not be resolved and therefore further test data was required.

This paper presents the performance of eccentrically loaded TWC columns with special reference to the performance of Volcanic Pumice Concrete (VPC) in a confined environment. Emphasis is provided on the use of locally available volcanic pumice, a natural waste from volcanic activities in Papua New Guinea to manufacture in-fill lightweight concrete (VPC). To the author’s knowledge little or no literature on lightweight VPC filled columns apart from current research study, is available. The performance of lightweight VPC in a confined environment as infill in TWC columns compared with normal concrete (NC), is an interesting aspect of this research. The lower modulus of elasticity of VPC (Hossain 1997) compared with NC can change the load-deformation characteristics of TWC columns.

The findings of this research will introduce the use of VPC and explore the viability of lightweight construction in Papua New Guinea and other volcanic areas. Development of design guidelines for TWC columns with both VPC and NC in-fill from experimental and design-oriented analyses is the aim of the current study.

1.1 Research significance

Due to frequent volcanic eruption, volcanic debris such as: volcanic ash and pumice are found abundantly in Papua New Guinea. The 1994 volcanic eruption that occurred in the East New Britain province completely devastated the province and created an environmental disaster. This research is put forward with the support from local industries to explore the utilization of volcanic debris in construction that can not only provide low cost cement and concrete but also can help to decrease environmental hazards.

Comprehensive research (Hossain 1997, 1999a,b) had been conducted on the use of volcanic ash (VA) and pumice (VP) in cement and concrete production. Recommendations and a patent have been developed for the local cement industry, ready mixed concrete companies and other construction industries to manufacture blended cement and concrete. Extensive research (Hossain 1998, 1999a, 2000, 2001) also led to the development of a novel form of thin walled composite (TWC) structural elements using volcanic ash and pumice based cement and concrete. These elements can be used to build houses and other utility structures especially suitable for rehabilitation project, in earthquake prone areas.

2. Experimental investigations

A comprehensive series of experimental investigation were conducted to study the behaviour of TWC columns employing VP based concrete. The experiments were designed to provide information on the load-deformation response, stress-strain characteristics and failure modes.

2.1 Descriptions and instrumentation

TWC columns were manufactured using commercially available hollow steel sections available in the market and also using flat sheet folded to hollow sections in-house with welded seam joints. The

Table 1 Details of eccentrically loaded columns

Column Designations	Column dimensions in mm							Material Properties		
	Sect.	*b*	*a*	*h*	*t*	*e*	*h/b*	Concrete		Steel
		Y	*X*	*Z*		e_y		$f'c$	f_{cu}	f_{sy}
								MPa		
E1nc, E1vpc, E1(unfilled)	SHS	50	50	900	1.6	25	18	28 (20)	38 (26)	275
E2nc, E2vpc	RHS	50	100	900	2.3	25	18	28 (20)	38 (26)	350
E3nc, E3vpc, E3(unfilled)	RHS	150	150	900	1.6	75	6	28 (20)	38 (26)	375

nc: normal concrete ; vpc: volcanic pumice concrete;
$f'c$ = concrete cylinder strength; f_{cu} = concrete cube strength
Values in the brackets are VPC strengths
E_s = 200000 N/mm^2; ε_{sy} = 0.0018 (average of coupon tests)
e, e_y: eccentricity = 0.5b; *X*, *Y*, *Z*: Reference axes (Fig. 1)

thickness of the steel varied from 1.6 mm to 3.2 mm. The dimensional properties of a typical column are indicated in Fig. 1, where *a* and *b* represent the cross-sectional dimensions with '*b*' representing minimum dimension; *h* and *t* represent the height of the column and thickness of the steel plate respectively.

The detailed descriptions of the columns are presented in Table 1. Three series of columns designated as E1, E2 and E3 were tested. The columns had equal heights with *h/b* ratios of 18, 18 and 6 for E1, E2 and E3 respectively.

According to clause 10.3.1 of AS 3600 (1988), a braced column may be regarded as short if $L_e/r \leq 60$, where L_e is the effective height and *r* is the radius of gyration (= 0.3*b*). All the columns tested in this study can be considered as braced. The series E1 and E2 can be classified as slender while series E3 as short.

All three sets of columns were tested at an eccentricity (e) of *b*/2. Testing with such large eccentricity may be impractical but the tests provided useful information on the strength and failure characteristics of columns under the dual influences of secondary moment due to P - δ effect and primary moment. It is important to note that the initial eccentricity (e) plays an important role on the behaviour of slender columns. The fall-off in strength with increasing slenderness is less severe when *e* is large. In such cases the primary moment is relatively large, and the secondary moment is a relatively small proportion of the total moment, and therefore less significant. As a result, material failure occurs in the critical section at mid-height, with little loss in strength, even for a very slender column. The fall-off in strength with increasing slenderness is most severe at small eccentricity. In such case, the peak load is reached without a material failure and a stability failure occurs due to the development of large secondary moment (Warner *et al.* 1997). To avoid a stability failure and to ensure a material failure (where the strength of the column section is exhausted), tests were conducted with comparatively large eccentricity.

2.2 Casting, curing and instrumentation of the columns

The infill concrete for VPC and normal concrete (NC) TWC columns were made from 10 mm maximum size VP and stone aggregates respectively. The columns were cast vertically in a specially fabricated stand and concrete was compacted in layers. The concrete was machine mixed, manually poured and vibrated with a portable poker vibrator. The behaviour of thin steel sheeting as formwork under wet concrete was observed during the casting operation and no sign of outward buckling in the sheeting was observed. Control specimens in the form of cubes and cylinders were also cast for each batch of concrete. The TWC column specimens were then air cured at room temperature until they were tested. The control specimens were removed from the moulds after 24 hours of casting and also air cured at room temperature.

The tensile strength (f_{sy}), modulus of elasticity (E_s) and yield strain (ε_{sy}) of the steel were determined from coupon tests. The steel and concrete properties of the TWC columns are presented in Table 1. The density of VPC and NC were about 1800 kg/m^3 and 2500 kg/m^3 respectively.

2.3 Instrumentation of column specimens

The strain gauges were installed at strategic locations (Fig. 1) to monitor axial (Gauges 1 to 4) and horizontal or hoop (Gauge 5) strain development in the steel. Gauge 1 was installed at a distance of 50 mm from the top while gauges 2, 3, 4 and 5 were placed at mid-height (0.5 h). Gauges 1, 2 and 5 were installed on the compressive face while gauge 3 was installed on the face adjacent to the tensile and compressive faces. Gauge 4 was placed on the tension face opposite to the loaded face.

2.4 Test set-up

All the columns were tested in a hydraulic testing machine and eccentric loads were applied through a specially designed and fabricated test setup as shown in Fig. 2.

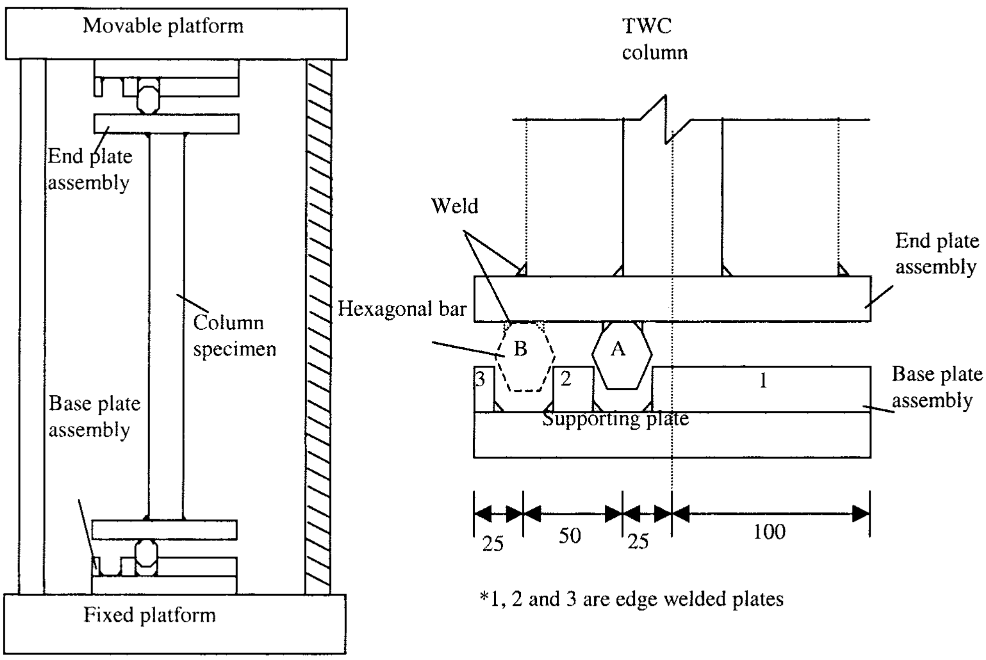

Fig. 2 Schematic of eccentric test set-up

The eccentric test setup consisted of a pair of end and base steel plate assembly with welded hexagonal rod and groove arrangement. The hexagonal rods were used because of the non-availability of large diameter round bars at the time of fabrication. The hexagonal rod and groove arrangement provided satisfactory interlocking and gripping during testing. The end plates were made of 20 mm thick and 200 mm square plate with a hexagonal bar welded at the eccentricities of 25 mm and 75 mm according to the required planned eccentricity. The end plates were welded to the ends of the column specimens before testing. The base plate arrangement consisted of three edge plates welded to a 20 mm thick supporting plate (200 mm square) that provided two 25 mm groves for hexagonal rod as shown in Fig. 2, allowing the load to be applied with 25 mm and 75 mm of eccentricity.

The end plate arrangement with welded bar was changed for each eccentric loading by cutting and shifting the bar as required for each column tested. The welded rod at the end plates were shifted to position A (Fig. 2) for E1 and E2 columns and to position B for E3 columns.

The columns were placed between the loading plates of the hydraulic testing machine. The base plate at the foot of the wall was firmly secured to the fixed base platform of the hydraulic testing machine to avoid slipping during eccentric application of load. Similarly the base plate at the top of the column was firmly secured to the top moving platform of the machine with specially designed welded rod-plate-bolt assembly.

The load was applied in increments and at each load increment, strains and deformations were recorded using electronic strain measuring equipment and dial gauges. General behaviour including cracking of concrete, buckling of sheeting and failure modes were also observed. Vertical and horizontal dial gauges were used to monitor axial and lateral (mid-height) displacements.

2.5 Experimental observation and failure modes

All eccentric columns showed sign of global buckling as loading continued. The load (P) increased with the increase of axial (Δ) and lateral (δ) deformations. The lateral deformation induced secondary moment due to P-δ effect in addition to primary moment in the post global buckling stages of the columns. The columns failed when significant global buckling associated with lateral deformation lead to the development of local buckle around the centre of the column. The formation of local buckling induced compression on the inward face and tension on the outward face of the column. The inward buckling of the compression steel plate was resisted by the infill concrete and forced the steel plate to buckle outward. The sheet-concrete interaction significantly increased the buckling capacity of the members. Finally, the column failed when the zone of local buckling created a plastic hinge that exhausted the strength of the column section. The typical failure mode of an eccentrically loaded column is shown in Figs. 3(a)-(b).

For E3 columns, local buckling was observed at the top but the failure load was governed by the global buckling with the development of plastic hinge at the centre of the column. The tearing sound of welded steel seam connection in E3 columns was heard only after the post failure stage.

The failure loads of the unfilled columns (E1 and E3) were governed by the local inward buckling (Fig. 3b) of the compression plates. The local buckling, quickly transformed into a plastic hinge due to absence of infill concrete. Comparatively slender column E1 failed due to the formation of local plastic hinge associated to global buckling. While short column E3 failed due to instability at the local buckles without much global buckling.

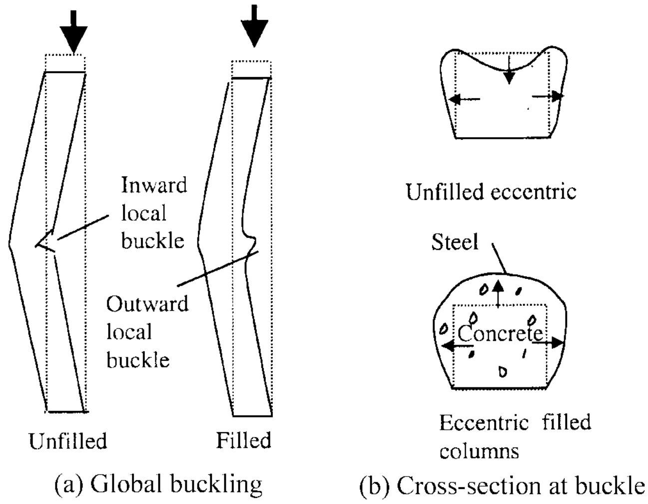

Fig. 3 Failure modes of the TWC columns

2.6 Comparison of load deformation response

The load-deformation responses for the E-columns are shown in Figs. 4 and the findings are summarized in Table 2. VPC and NC columns showed similar load-deformation response with VPC columns producing lower strength.

4 to 5% loss of strength in VPC columns (in series E1 and E2) compared with NC columns as shown in Table 2 seems to be good enough when performance is considered based on the lower strength of VPC (about 30% lower). This is an indication of the effective confinement enhancing the performance of low strength VPC. Such lower strength loss may also be due to the relatively thicker

Table 2 Comparative study of eccentric column performance

Eccentric Columns			
Name	Load	Deformation (Def.)	
	P kN	Δ mm	δ mm
E1nc	80.4	6.33	14.36
E1vpc	76 (–5%)	5.50 (–13%)	13.25 (–8%)
E1	36	2.66	----
E2nc	214	8.69	19.29
E2vpc	206(–4%)	6.01 (–31%)	14.81 (–23%)
E3nc	414	17.7	14.63
E3vpc	320(–23%)	20.2 (+14%)	10.90 (–25%)
E3	62	2.0	1.11

P: Ultimate eccentric load; Δ, δ: Axial and lateral deformation at ultimate load respectively
Values in brackets represent % increase or decrease in load and deformation in VPC columns compared with NC columns

steel tubes and smaller contribution of concrete (smaller cross-sectional area) to the overall strength. On the other hand, 23% lower strength of column E3vpc compared with column E3nc may be due to the following reasons:

- thin steel tubes and high concrete contribution due to bigger cross-sectional area compared to E1 and E2 lead to the higher effect of VPC.
- weaker VPC underwent more deformation and failed at lower load causing more stress concentration on the steel skin
- thin steel sheet with welded seam connections under stress concentration aggravated the failure

Tests suggest that the degree of confinement depends on the thickness of the steel tube as well as dimension, slenderness and eccentricity of columns.

The axial and lateral deformations at ultimate load are found to be less (as indicated in Table 2) in VPC columns compared with NC columns.

The graphs showing the variation of lateral deformation (δ) with axial load (P) in eccentric columns are superimposed on the axial load (P)-axial deformation (Δ) responses in Figs. 4(b)-(d). It is found that the eccentric columns underwent significant lateral deformation due to global buckling and plastic hinge formation before failure.

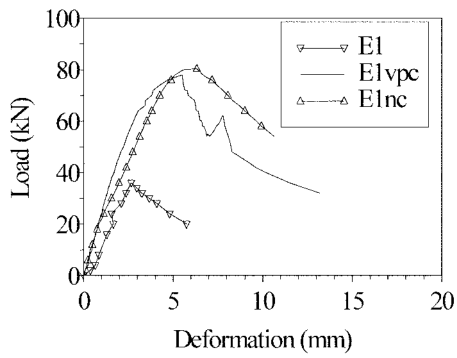

Fig. 4(a) Development of axial deformation in eccentric columns

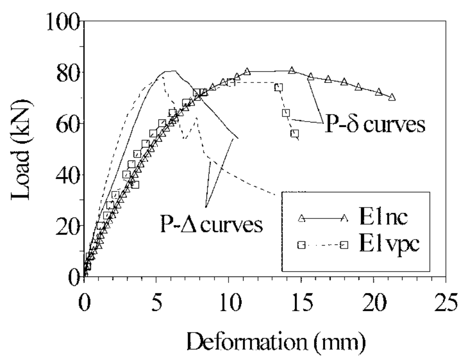

Fig. 4(b) Development of axial and lateral deformatio in eccentric columns

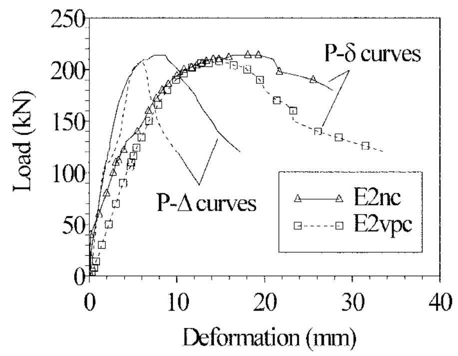

Fig. 4(c) Development of axial and lateral deformation in eccentric columns

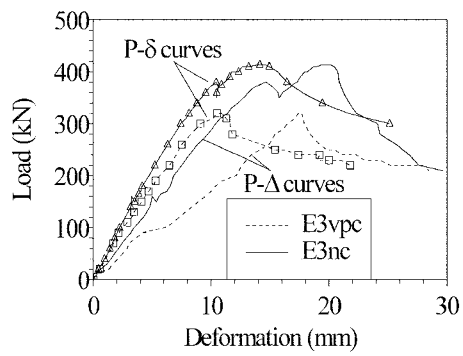

Fig. 4(d) Development of axial and lateral deformatic in eccentric columns

The strength of the eccentrically loaded TWC columns decreased with an increase in slenderness ratio while they were loaded with equal relative eccentricity (= 0.5*b*).

Typical load-deformation response of the unfilled column (E1) is superimposed on those from filled columns in Fig. 4(a). The strength of the unfilled column (Table 2) was only 15% (NC) and 19% (VPC) of short filled columns in series E3 while 45% (NC) and 47% (VPC) of slender filled columns in series E1. The strength of the unfilled section was found to be dependent on the mode of failure, cross-sectional dimensions and *b/t* ratios.

2.7 Strain characteristics

The variation of strain in VPC and NC eccentric columns (E1nc and E1vpc) is shown in Figs. 5. The strain gauges 1 and 2 on the loaded face were predominantly subjected to compressive strains as expected while strain gauge 4 on the unloaded face was subjected to tensile strain in both NC and VPC columns. This was due to the development of uniaxial bending moment in the columns. Gauge 1 was yielded at about 62% and 68% of ultimate load for NC and VPC columns respectively. Gauge 2 was yielded at about 75% and 68% of ultimate load for NC and VPC columns respectively. In general, compressive strain in gauge 1 and gauge 2 for both NC and VPC columns showed a similar behaviour.

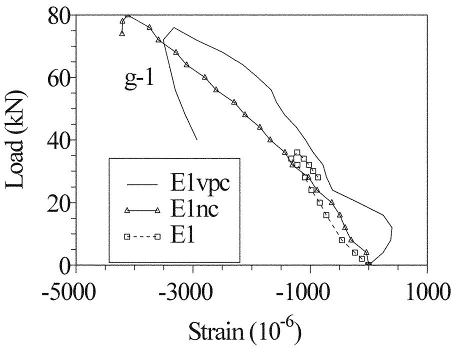

Fig. 5(a) Strains in eccentric columns E1

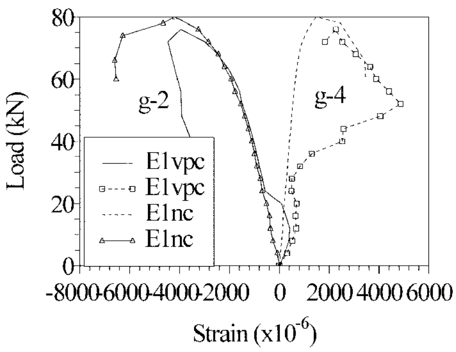

Fig. 5(b) Strains in eccentric columns E1

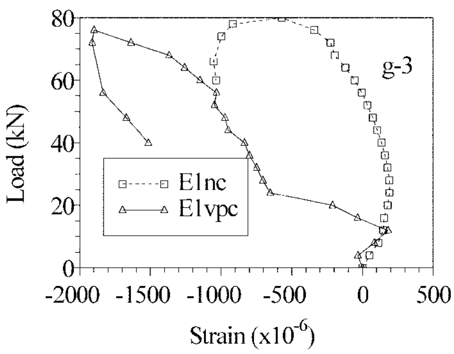

Fig. 5(c) Strains in eccentric columns E1

The strain gauge 3 was installed at the centre of the transverse face of the columns. The variation of strain showed a compressive behaviour at progressive loading although it showed a tensile behaviour in the early stages. The transition from tensile to compression strain might be due to the change in the interaction between steel and concrete. But the gauges were not yielded.

The tensile strain in gauge 4 of VPC column exceeded the yield strain at much earlier load (51% of ultimate load) than its NC counterpart where yielding was observed after the ultimate load. This might be due to the formation of plastic hinge directly at mid height of the VPC column (where gauge 4 is located) compared with NC column where it formed below the mid height.

Fig. 5(a) compares the strain in gauge 1 for unfilled steel section (E1) with those from NC and VPC columns. It can be seen that gauge 1 in all three columns are under compression. It is interesting to note that the unfilled steel section failed due to global buckling but did not register yield strain in gauge 1 as observed in the case of filled columns. It might be due to the localised inward buckling (Fig. 3c) of the compression steel plate at plastic hinge formed due to global buckling of unfilled steel section at mid height. In the case of TWC columns, inward buckling of the compression steel plate was resisted by concrete infill and forced the plate to buckle outward (Fig. 3c). This resulted in better redistribution of stresses along the height of the column. As a result, strain gauges at both top and mid height of the column registered yield strain.

3. Proposed analytical model for eccentric columns and development of strength interaction diagram

An analytical model for eccentric columns (Hossain 2001) is formulated based on AS3600 (1988) with modification taking into consideration of the effect of confined concrete. The concrete cylinder strength ($f'c$) used in AS 3600, is replaced by the confined concrete strength (f_{cc}) in the proposed model.

For a TWC column subjected to either concentric or eccentric loading conditions, the interactive confinement will not occur until the concrete begins yielding, since at the initial stage of loading the steel tube has much higher Poisson's ratio and laterally dilates much more than the concrete. After yielding, the concrete shows nominal Poisson's ratio greater than 0.5 and laterally expands outward more than the steel tube. As a consequence, the steel tube, subjected to bi-axial tension-compression, will confine "extra" dilatation of the filled concrete. Due to containment effect of steel tube, the filled concrete is under tri-axial compression and becomes the so-called confined concrete. The state of stress in a TWC circular column is shown in Fig. 6(a).

Following Sun *et al.* (1998), the yield criterion for the confined concrete and the steel tube generally can be written as follows:

$$f_{cc} = f_p + 4.1 f_l \tag{1a}$$

$$\sigma_{sz}^2 - \sigma_{sz}\sigma_{sh} + \sigma_{sh}^2 = f_{sy}^2 \tag{1b}$$

where f_p is the unconfined concrete strength, f_l is the lateral pressure from the steel tube at the peak stress f_{cc}, σ_{sz} and σ_{sh} are the axial stress and hoop stress of steel tube, respectively, and f_{sy} is the uniaxial yield stress of steel. Note that the peak stress of concrete may be assumed correspondent with the peak load of the TWC column because the yield of steel tube generally occurs before the

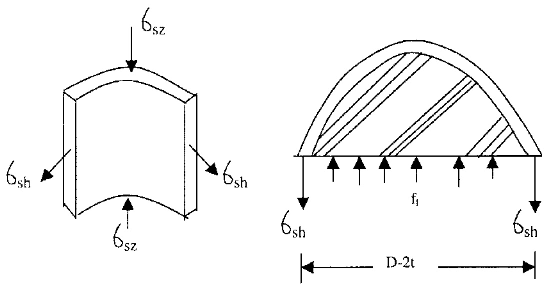

Fig. 6(a) Confinement effect in TWC column

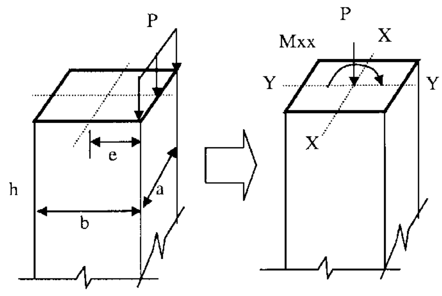

Fig. 6(b) Loading of eccentric columns

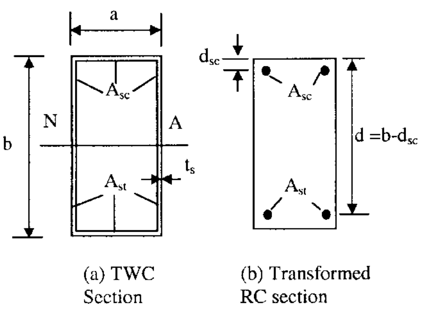

Fig. 6(c) Transformation of TWC Columns

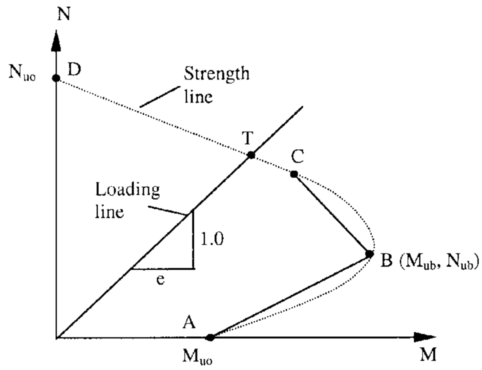

Fig. 6(d) Interaction diagram

yield of concrete. The lateral pressure (f_l) can be obtained by Eq. (1c) through the equilibrium condition shown in Fig. 6(a).

$$f_l = \frac{2t}{D-2t}\sigma_{sh} \tag{1c}$$

where D and t are diameter and thickness of the confining steel tube in case of circular section.

Square or rectangular sections are to be transformed into equivalent circular section. As obvious from Eqs. (1a)-(1c), to completely determine the confinement effect, i.e. the confined concrete strength f_{cc}, the value for hoop stress σ_{sh} in steel tube at the peak load is necessary. At the initial stage of loading, only axial compressive stress is developed in the steel tube. After the axial stress reached uniaxial yield stress, f_y, hoop tensile stress is induced in the steel tube following the Von Mises yield curve. With the increase of axial deformation, the hoop stress increases while the longitudinal stress decreases. Both stresses σ_{sz} and σ_{sh} will converge to certain values αf_y and βf_y, respectively, when the axial strain becomes five times or more of the uniaxial yield strain.

Analysis of axial and hoop stresses developed in the TWC columns with NC and VPC in the current study suggests that the value of α should be ranged between 0.18 and 0.24 for concentric while between 0.16 and 0.20 for eccentrically loaded columns (Hossain 2000, 2001). The eccentricity and slenderness of the columns seem to lower the value of α and hence have the effect of reducing the confinement as suggested in Eurocode 4 (1993). A constant value of 0.19 is assumed in the current study for the parameter α in deriving the equation for f_{cc}. The assumed value of α is similar to that recommended by AIJ (1997) design guideline based on a statistical analysis on the test results of columns under concentric loading.

Substituting $\sigma_{sz} = \beta f_{sy}$ and $\sigma_{sh} = \alpha f_{sy}$ and $\alpha = 0.19$ into Eq. (1b), one can obtain $\beta = 0.89$. Then the confined concrete strength (f_{cc}) can be derived as a function of the cross-sectional dimension of the column and yield strength of the confining steel (f_{sy}) as shown in Eq. (1d).

$$f_{cc} = f_p + 4.1 f_l = f_p + 4.1\frac{2t}{D-2t}\alpha f_{sy} = f_p + \frac{1.56}{D/t-2} f_{sy} \tag{1d}$$

For rectangular and square sections, the value of D can be calculated by converting these sections into equivalent circular sections (Hossain 2000, 2001). The value of f_p can be taken as $0.85f'c$ for 100 mm diameter standard cylinder. To maintain wide applicability and to take into account the size effect of column on the f_p, Eq. (1e) is proposed to calculate f_p (Sun *et al.* 1998):

$$f_p = 1.61(d)^{-0.1} f'_c \tag{1e}$$

where d is the diameter of concrete section in mm and $f'c$ is the compressive strength of 100 mm diameter standard cylinder in MPa. AIJ (1997) design guideline based on a statistical analysis on the test results of columns suggested: $\alpha = 0.19$ and $\beta = 0.89$.

TWC column shown in Fig. 6(b) is transformed into an equivalent reinforced concrete (RC) section as shown in Fig. 6(c). In transforming the section, the steel area above the neutral axis is designated as compressive steel (A_{sc}) and that below the neutral axis is designated as tensile steel (A_{st}). Both compressive and tensile steels are lumped at the centroid of their respective half sections at depths d_{sc} and $b\text{-}d_{sc}$ from the top extreme concrete fibre respectively. Also due to the symmetry of the section, the plastic centroid (d_p) is situated at mid-height ($0.5b$) of the section and hence $A_{st} = A_{sc} = bt + at$.

3.1 Proposed strength equations- tension over part of section (Region CA)

The analysis for strength varies according to the distribution of strain in the section. We first consider region CA of the interaction diagram of Fig. 6(d) for which there is some tension in the tensile steel. Conditions showing the state of stress, strain and force systems in the section are shown in Fig. 7.

Using the equivalent rectangular stress block concept, the compression force (C_c) in the concrete can be written as: $C_c = 0.85\gamma f_{cc} a k_{ud}$. The value of γ can be calculated by using: $\gamma = 0.85 - 0.007 (f'c\text{-}28)$ with the limits $0.65 < \gamma < 0.85$ (based on AS 3600).

The force in the compressive steel (C_s) is: $C_s = \sigma_{sc} A_{sc}$ and the force in the tensile steel (T) is: $T = \sigma_{st} A_{st}$

Steel stresses are expressed as σ_{sc} and σ_{st} because it is not known at this stage of the analysis whether either or both steels are at yield.

For equilibrium, the three internal forces must add up to the applied load, N_u:

$$N_u = C_c + C_s - T \tag{2}$$

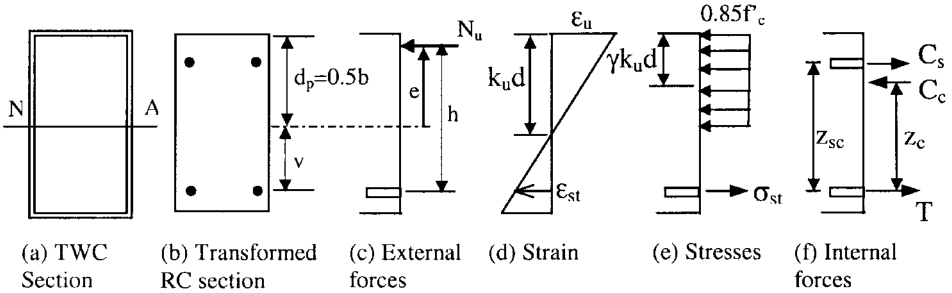

Fig. 7 Stress-strain characteristics of TWC column subjected to eccentric load

The additional requirement is expressed by taking moments (Fig. 7) of internal and external forces about the level of the tensile steel.

$$N_uh = C_cz_c + C_sz_s \tag{3}$$

The lever arm z_c is obtained from the fact that C_c acts at depth, d_c = 0.5 $k_u d$ below the top surface: $z_c = d(1 - 0.5\ \gamma k_u)$. The other lever arm $z_{sc} = d - d_{sc}$. Substitution of appropriate expressions into the equilibrium Eqs. (2) and (3) leads to the following equations:

$$N_u = 0.85\gamma f_{cc}adk_u + \sigma_{sc}A_{sc} - \sigma_{st}A_{st} \tag{4}$$

$$N_uh = 0.85\gamma f_{cc}ad^2k_u(1 - 0.5\gamma k_u) + \sigma_{sc}A_{sc}[d - d_{sc}] \tag{5}$$

It can be noted that h is measured from the level of the tensile steel, whereas moment (M) is defined in terms of the eccentricity, e, measured from the plastic centroid. If v is the distance from the tensile steel to the plastic centroid, the ultimate moment (M_u) can be calculated as:

$$M_u = N_u(h - v) \quad \text{and} \quad e = h + v$$

Each point on the portion CA for the strength line of Fig. 6(c) corresponds to a particular value of k_u. For a chosen value of k_u less than 1.0, the steel strains may be calculated from strain diagram shown in Fig. 7 as:

$$\varepsilon_{st} = \varepsilon_u\frac{1 - k_u}{k_u}, \quad \varepsilon_{sc} = \varepsilon_u\frac{k_u - d_{sc}/d}{k_u} \tag{6}$$

where ε_u = ultimate compressive strain of concrete = 0.003.

If the tensile (ε_{st}) and compressive (ε_{sc}) strains are less than the steel yield strain (ε_{sy}), the corresponding stresses in steel can be calculated as $E_s\varepsilon_{st}$ or $E_s\varepsilon_{sc}$; otherwise the steel stress can be taken as yield stress (f_{sy}). Eqs. (4) and (5) can be used to calculate corresponding values N_u and M_u which are the co-ordinates of a point on the strength curve (Fig. 6c).

3.2 Balanced failure (Point B)

At the balanced failure, the tensile steel strain is ε_{sy} and the tensile steel stress is f_{sy}. The compressive steel strains will usually exceed ε_{sy}, so the compressive steel stress will also be f_{sy}. The factor k_{ub}, defining the neutral axis position, can be derived from strain diagram as:

$$k_{ub} = \frac{\varepsilon_u}{\varepsilon_u - \varepsilon_{sy}}$$

The balance load N_{ub} and balance moment M_{ub}, representing point B on the interaction diagram, can be calculated by substituting k_{ub} in Eqs. (4) and (5):

$$N_{ub} = 0.85\gamma f_c' a d k_{ub} + f_{sy}(A_{sc} - A_{st}) \tag{7}$$

$$N_{ub} h_b = 0.85\gamma f_c' a d^2 k_{ub}(1 - 0.5\gamma k_{ub}) + f_{sy} A_{sc}(d - d_{sc}) \tag{8}$$

$$M_{ub} = N_{ub}(h_b - v) \tag{9}$$

3.3 Primary tension failure (Part AB)

When 'e' is larger than the balanced eccentricity (e_b), the tensile steel is at yield and σ_{st} is set equal to f_{sy} in Eqs. (4) and (5). The parameter $k_u < k_{ub}$ and the Eqs. (4) and (5) refer to the part AB of the interaction diagram. The compressive steel may or may not be at yield, depending on the location of the neutral axis.

The abscissa M_{uo} for the point A can be approximated by using the following two equations:

$$M_{uo} = A_{sc} f_{sy}(d - d_{sc}) + 0.85\gamma f_{cc} a d k_u (d - 0.5\gamma k_u d) \quad \text{where} \quad k_u = \frac{(A_{st} - A_{sc}) f_{sy}}{0.85\gamma a d f_{cc}} \tag{10}$$

$$M_{uo} = A_{st} f_{sy}(d - d_{sc}) \tag{11}$$

Eq. (10) should be used when both A_{st} and A_{sc} are yielded and Eq. (11) when A_{sc} is not yielded.

3.4 Primary Compression Failure (PCF) (Part BC)

When 'e' is less than e_b, the stress in the tensile steel is less than f_{sy}. The steel strain ε_{st} is obtained from Eq. (6) and the stress (σ_{st}) = $E_s \varepsilon_{st}$. The compressive steel stress will be f_{sy}. The parameter $k_u > k_{ub}$ and the Eqs. (4) and (5) can be used to simulate the part BC of the strength line.

3.5 Compression over whole section (Part CD)

When $ku > 1.0$, both compressive and tensile steels are in compression. Indeed, if $k_u >$ about 1.1 the whole section is in compression. The portion CD of the strength curve can be approximated with good accuracy by a straight line. The ordinate N_{uo} for point D can be obtained from the proposed axial capacity of TWC column (Hossain 2000) by superimposing the axial capacity of confined concrete section on that carried by steel portion:

$$N_u = \beta A_s f_{sy} + A_c f_{cc} \approx A_c f_p \left[1 + (4\beta + 8.2\alpha) \frac{t}{D - 2t} \frac{f_{sy}}{f_p} \right] \tag{12}$$

where A_s and A_c are the area of steel portion and filled concrete section, respectively.

The corresponding axial capacity of TWC columns can be calculated based on AS3600 (1988), assuming material safety factors to be equal to unity, from the following equation:

$$N_u = A_s f_{sy} + 0.85 f_c' A_g \tag{13}$$

where A_g is the gross cross-sectional area of the column. Following the procedure described above, complete strength line ABCD for eccentrically loaded TWC columns can be constructed as shown by dashed line in Fig. 6(c).

3.6 Development of computer program to generate interaction diagrams and for the determination of strength

A computer programme is developed to generate the interaction diagrams for TWC columns based on the proposed design equations. The intersection point '*T*' (as shown in Fig. 6c) of the loading line and the strength line represents the strength of the column for a particular eccentricity.

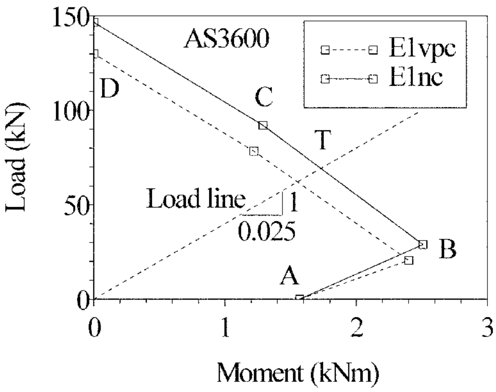

Fig. 8(a) Comparison of interaction diagrams for both NC and VPC columns

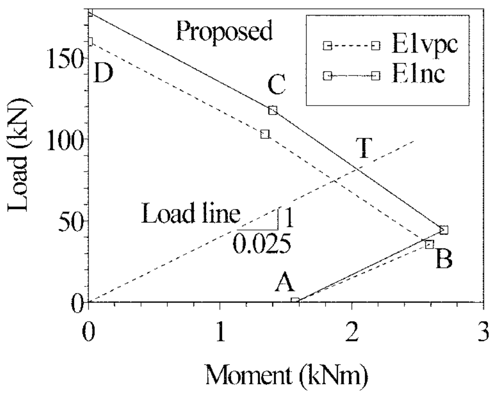

Fig. 8(b) Comparison of interaction diagrams for both NC and VPC columns

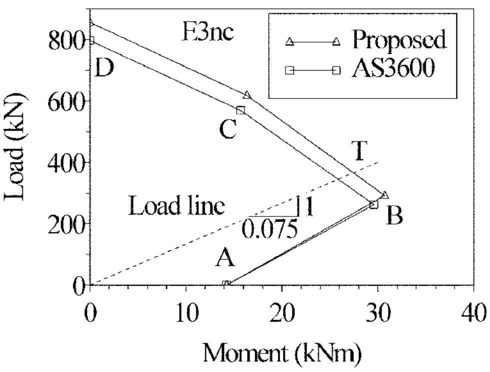

Fig. 9(a) Comparison of interaction diagrams

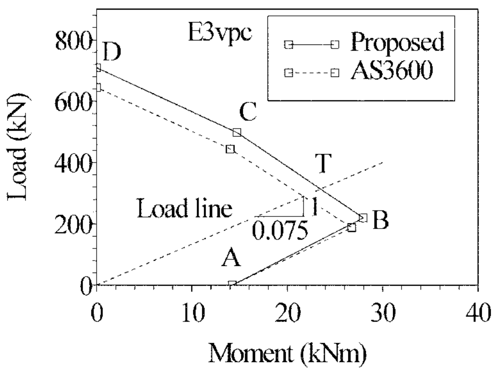

Fig. 9(b) Comparison of interaction diagrams

Table 3 Comparative study of experimental and analytical predictions

Column	Theory								Expt.		Ratio		Remark
	AS3600				Proposed Model				P	M_{xx}	Expt/Theory		Failure
	f'_c MPa	P kN	M_{xx} kNm	e_b mm	f_{cc} MPa	P kN	M_{xx} kNm	e_b mm	kN	kN.m	Proposed	AS3600	Type
E1nc	28	70	1.72	87	43	81	2.05	61	80.4	2.01	0.99	1.15	PCF
E1vpc	20	62	1.52	117	34	74	1.87	73	76.0	1.90	1.03	1.23	PCF
E2nc	28	172	4.23	113	46	200	5.00	74	214	5.35	1.07	1.24	PCF
E2vpc	20	158	3.92	124	37	185	4.68	88	206	5.15	1.11	1.30	PCF
E3nc	28	346	25.6	113	31	370	27.2	105	414	31.05	1.12	1.20	PCF
E3vpc	20	290	21.6	143	23	318	23.5	128	320	24.00	1.01	1.10	PCF

e_b: balanced eccentricity, P: Eccentric load, M_{xx}: Moment, PCF: Primary Compression Failure

The interaction diagrams for E1, E2 and E3 columns are generated using both AS3600 and the proposed method and typical results (for columns E1nc, E1vpc, E3nc & E3vpc) are presented in Figs. 8(a)-(b) & 9(a)-(b).

Figs. 8(a)-(b) compare the typical interaction diagrams for NC and VPC columns. AS3600 uses characteristic cylinder strength of concrete (f'_c) while the proposed method uses confined strength of concrete (f_{cc}). VPC columns showed lower strength compared with NC columns. This may be partially attributed to the lower strength of VPC compared with NC. Table 3 compares the performance of the proposed method.

All the columns are predicted to undergo (as indicated in Table 3) primary compression failure (both AS3600 and Proposed) as the point '*T*' lies in the zone BC of the strength line (Figs. 8a-b & 9a-b).

Figs. 9(a)-(b) compare the performance of the proposed and AS3600 methods. It is found that AS 3600 under predicts the capacity of TWC columns compared to proposed method as it does not use the strength enhancement of confined concrete. The proposed method provides better prediction as the ratio of experimental to predicted strength remains very close to unity (Table 3). The proposed method can therefore be used with confidence for the design of both VPC and NC TWC columns subjected to eccentric load.

4. Conclusions

The behaviour of eccentrically loaded filled TWC columns highlighting the performance of VPC compared with normal concrete in a confined state is described based on experimental and design oriented analyses. The capacity of the columns is based upon the increased strength of confined concrete and the increased steel plate buckling capacity due to composite action. Analytical models taking into consideration of confinement effect are formulated for both axial and eccentric loading conditions to develop strength-interaction diagrams. The performance of the proposed design method is validated from experimental and Code based models. The following conclusions are drawn from the study:

- All eccentric columns failed when a zone of local buckling around column mid-height, created a plastic hinge that exhausted the strength of the section. This was also associated with significant global buckling and excessive lateral deformation. The tearing of welded steel seam connection in columns made in-house (E3) was observed only after the post failure stage.
- VPC and NC columns showed similar load-deformation responses. Only 4 to 5% loss of strength in VPC columns compared with NC columns was an indication of good performance considering a 30% lower strength of VPC compared to NC. This was also an indication of effective confinement enhancing the performance of low strength concrete in TWC columns.
- A 23% lower strength (in-house made columns) of E3vpc compared with E3nc might be due to weaker VPC and weakness in the welded seam connection causing lower confining effect.
- The axial and lateral deformations at ultimate load seemed to be less in VPC columns compared with NC columns.
- The strengths of the eccentrically loaded columns were found to be only 49% to 54% of the corresponding similar axially loaded columns (Hossain 2000, 2001). Ultimate axial deformations in eccentrically loaded columns were found to be higher (ratio of axial deformation varies from 1.24 to 3.05) than axially loaded columns. Such reduction in strength was due to the testing of such columns with large eccentricity that induced a large uniaxial bending moment. This may be the case of an external column in a building subjected to cantilever beam action. However, Clause 10.1.2 of AS 3600 requires that a minimum bending moment (equivalent to the applied load times an eccentricity of 0.05 times the overall dimension of the section in the direction of bending) about each principal axis be considered in the design of any column. Clause 10.3.3 of AS 3600 also allows the moment (if it is small) to be disregarded provided the design strength of the cross-section is reduced to $0.75N_u$. Current tests on TWC columns with large eccentric application of load provided information under worst possible situation. The strength of TWC columns will be much better under minimum bending moment suggested by Clause 10.1.2 of AS 3600.
- In the case of TWC columns, inward buckling of the compression steel plate is resisted by concrete infill and forced the plate to buckle outward. This resulted in better redistribution of stress along the height of the column compared to individual steel column. This resulted in yielding of steel at both top and mid height of the columns.
- Analytical model for the eccentric column is formulated based on AS3600 (1988) with modification taking into consideration of the effect of confined concrete using confined concrete strength f_{cc} and replacing TWC columns with an equivalent RC section. The effect of the type of concrete (VPC or NC) as well as slenderness and eccentricity of columns on the confinement is taken into account with the introduction of two parameters α and β whose values are suggested based on experimental results.
- AS 3600 under predicted the capacity of TWC columns by about 25% as it did not consider the strength enhancement of confined concrete. The proposed method provided better prediction as the ratio of experimental to predicted strength remained very close to unity.
- A computer programme is developed to generate the interaction diagrams for TWC columns based on the proposed model with its performance validation based on AS3600.
- The proposed method can be used with confidence for the design of both VPC and NC TWC columns subjected to eccentric load.
- The performance of VPC in TWC sections is found satisfactory and in future, volcanic pumice can be used as a potential source of alternative aggregate. The 30% lighter VPC (compared to

NC) satisfies the criteria for structural lightweight concrete (Hossain 1999b) and its use will greatly reduce the weight of structural elements. Such lightweight structural elements with VPC are highly desired in earthquake prone areas.

Acknowledgements

The author is grateful to the Papua New Guinea University of Technology for providing financial assistance in this project. The author is also grateful to the Technical staffs of the Central Engineering Workshops, Structure & Material laboratories of the Department of Civil Engineering. Sincere thanks to Mr. L. T. Kovi Mol, Research Assistant associated with this project, The PNG Halla Cement Factory and BHP steel Ltd for their assistance.

References

Architectural Institute of Japan (AIJ) (1997), Recommendation for Design and Construction of Concrete Filled Steel Tubular Structures, October.

AS 3600 (1988), Standard Association of Australia: Concrete Structures.

BS 5400 (1979), Steel, Concrete and Composite Bridges: Part 5: Code of Practice for Design of Composite Bridges, British Standard Institution.

BS5950, Part 1 (1988), Introduction to Steel Work Design, The Steel Construction Institute, UK.

Eurocode 4 (1994), Design of Composite Steel Concrete Structures: Part 1.1. General Rules and Rules for Buildings, DD ENV 1994-1-1, BSI, London.

Hossain, K.M.A. (1997), "Development of mix-design charts for volcanic ash and pumice concrete", Research Report No. CE-SE97-5, Department of Civil Engineering, University of Technology, Lae, Papua New Guinea.

Hossain, K.M.A. (1998), "Behaviour of thin walled composite sections as structural elements", *Proc. of the Australasian Structural Engineering Conference*, Auckland, 30 Sept. - 2 October, **1**, 175-180. (ISBN 0-473-05481-7).

Hossain, K.M.A. (1999a), "Performance of volcanic pumice concrete with especial reference to high-rise composite construction", Innovation in Concrete Structures: Design and Construction, Edited by R.K. Dhir and M.R. Jones, Thomas Telford Publishing, Thomas Telford Limited, London, UK, 365-374, September. (ISBN 0 7277 28245).

Hossain, K.M.A. (1999b), "Properties of volcanic ash and pumice concrete", IABSE Report, **80**, 145-150, (ISBN 974-331-139-4).

Hossain, K.M.A. (2000), "Behaviour of thin walled composite columns", Research Report No: CE-SE-00-1, Department of Civil Engineering, UNITECH, Lae, Papua New Guinea.

Hossain, K.M.A. (2001), "Performance of volcanic pumice based thin walled composite columns", *Proc. Int. Conf. on Composite Engineering 8 (ICCE/8)*, 367-368, August 5-11, Canary Islands, Spain.

Neogi, P.K., Sen, H.K. and Chapman, J.C. (1969), "Concrete filled tubular steel columns under eccentric loading", *The Structural Engineer*, **47**(5), May, 187-195.

Shakir-Khalil, H. and Mouli, M. (1990), "Further tests on concrete-filled rectangular hollow section columns", *The Structural Engineer*, **67**(19/3), October, 346-353.

Shakir-Khalil, H. and Zeghiche, J. (1989), "Experimental behaviour of concrete-filled rolled rectangular hollow-section columns", *The Structural Engineer*, **67**(19/3), October, 346-353.

Sun, Y.P. and Sakino, K. (1998), "Modelling for the axial behaviour of high strength CFT columns", *Proc. 23rd Conf. on our World in Concrete & Structures*, 25-26 August, 179-186, Singapore.

Wang, Y.C. (1999), "Tests on slender composite column", *J. Constructional Steel Research*, **49**(1), 25-41.

Wang, Y.C. and Moore, D.B. (1997), "Design method of concrete-filled, hollow section, composite columns", *The Structural Engineer*, **75**(21), November, 368-373.

Warner, R.F., Rangan, B.V. and Hall, A.S. (1997), *Reinforced Concrete*, 3rd Edition, Addison Wesley Longman Australia Pty Ltd.

Wright, H.D. (1993), "Local buckling of rectangular hollow sections", *5th Int.l Symp. on Tubular Structures*, Nottingham, 25-27 August.

Wright, H.D. (1995), "Local stability of filled and encased steel sections", *J. Struct. Eng.*, ASCE, **121**(10), 1382-1388.

Wright, H.D. and Hossain, K.M.A. (1995), "The behaviour of composite rectangular tubes under bending and axial loading", *Proc. of Nordic Steel Construction Conference*, 523-530, Malmo, Sweden.